# Localization of antifouling surface additives in the pore structure of hollow fiber PVDF membranes

Evdokia Oikonomou, Szilvia Karpati, Sana Gassara, Andre Deratani, François Beaume, Olivier Lorain, Sylvie Tencé-Girault, Sophie Norvez

# Localization of antifouling surface additives in the pore structure of hollow fiber PVDF membranes

Evdokia K. Oikonomou,[1] Szilvia Karpati,[1] Sana Gassara,[2] André Deratani,[2] François Beaume,[3] Olivier Lorain,[4] Sylvie Tencé-Girault,[1] and Sophie Norvez[1,*]

[1] Laboratoire Matière Molle et Chimie, ESPCI Paris, PSL Research University, 10 rue Vauquelin, 75005 Paris, France

[2] Institut Européen des Membranes, IEM, UMR-5635, Université de Montpellier, ENSCM, CNRS, Place Eugène Bataillon, 34095 Montpellier Cedex 5, France

[3] ARKEMA, Usine de Pierre-Bénite, rue Henri Moissan, 69310 Pierre-Bénite, France

[4] POLYMEM, 3 rue de l'industrie, 31320 Castanet Tolosan, France

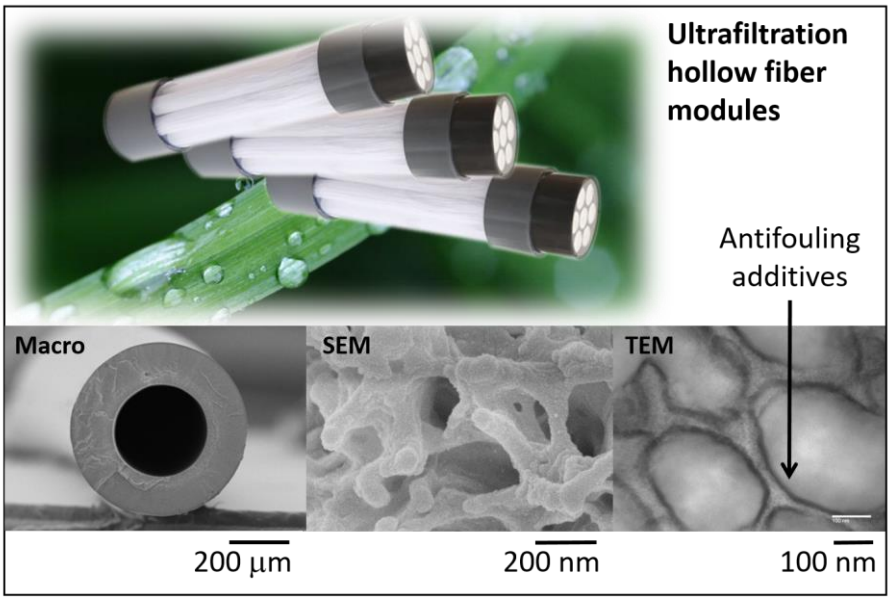


* sophie.norvez@espci.fr

## Abstract

Industrial hollow fiber membranes for the purification of wastewater were manufactured by the phase inversion method in a dry-wet spinning process, adding an amphiphilic diblock copolymer to a standard PVDF/Polyvinylpyrrolidone (PVP) formulation. The copolymer designed to provide antifouling properties is composed of a PMMA block and a hydrophilic block bearing pendent hydroxy groups. As PMMA is miscible with PVDF, the copolymer is expected to anchor in the matrix more efficiently than the hydrophilic but water soluble PVP which is washed away overtime during repetitive cleaning procedures.

Infrared experiments attest that both antifouling additives are well included in the fibers after the inversion process. Performances of the fibers were checked by permeability, burst pressure and tensile tests. The pore distribution observed by scanning electron microscopy goes from 10-30 nm at the outer surface to 0.1-10 μm inside the fiber. Observation of the pore structure by transmission electron microscopy, made possible by embedding the fibers into a resin that filled in the voids, and specific staining of the antifouling additives, shows that both PVP and the amphiphilic copolymer are located all around the pores. This study is the first direct proof at the microscopic scale of pore surface enrichment by antifouling agents.



**Keywords:** porous hollow fiber, PVDF, antifouling diblock copolymer, transmission electron microscope, pore structure.

## 1. Introduction

Poly(vinylidene fluoride) (PVDF) is a polymer commercially used for microfiltration and ultrafiltration membrane fabrication due to its excellent chemical resistance, high mechanical strength and thermal stability. However, its hydrophobic nature makes PVDF sensitive to fouling, which is a serious drawback for a widespread application in water treatment.[1,2] Fouling is a major issue in the long-term use of porous membranes for wastewater ultrafiltration. Organic matter, e.g. oil or proteins, are prone to adsorb onto hydrophobic membrane surfaces, leading to pore clogging and subsequent reduction of permeate flux, which results in increased operation cost and decreased service life of the membrane modules. Fouling resistance is improved by an increase of the membrane hydrophilicity, which favors the formation of a water layer preventing adsorption and deposition of hydrophobic pollutants.

Therefore, methods have been developed to enhance the hydrophilicity of PVDF membranes, which can be mainly classified into two categories, surface modification (by coating [3-5] or grafting[6-10]) and blending modification with hydrophilic polymers[11] or nanoparticles.[12,13] Coated layers have limited long-term stability with respect to removal during operation and aggressive cleaning procedures. Coating and grafting may result in modification of pore channels near the membrane surface. Moreover, surface grafting needs extra steps to modify the membrane surface, such as electron beam exposure, plasma treatment, UV photo-grafting or other living/controlled grafting methods.[14,15,10] Blending modification is a single-step method more adapted for industrial scale-up without pre- or post-treatment as encountered in surface modification. Water soluble polymers, in particular polyvinylpyrrolidone (PVP) or polyethylene glycol (PEG) derivatives, which additionally act as pore-controlling agents, are commonly used for blending with PVDF. The main drawback is that these hydrophilic additives are gradually washed away overtime resulting in decreased hydrophilic effect. Many amphiphilic copolymers with different chemistries and structures have been used to modify the PVDF hydrophilicity, mainly comb-like e.g. PVDF-g-PEGMA,[16,9] random P(MMA-r-PEGMA),[17,18] triblock,[19] block-like[20] or branched polymers.[21] The hydrophobic main chain segments exhibit a good compatibility with PVDF that delivers the long term stability of the copolymer in the membrane, while the hydrophilic side chain segments endow the membrane with the desirable hydrophilicity after surface segregation during the phase inversion process.

Among these amphiphilic additives, very few linear diblock copolymers have been reported,[22,23] and the localization of the active moieties in the porous matrix has never been demonstrated. Methods for measuring hydrophilicity or fouling mitigation, as for example contact angle measurement or static protein adsorption, give information on macroscopic properties only. On the other hand, Raman microscopy has been used to determine the PVP concentration profile along the cross-section radial axis of PVDF hollow fiber.[24] However, the spatial resolution of the method is limited to the micron scale. In this work, an amphiphilic diblock copolymer is used for blending modification of PVDF-based hollow fiber membranes. The first block is composed of PMMA compatible with PVDF, thus acting as an anchor for the copolymer in the matrix, and the second block possesses an acrylate backbone (polybutylacrylate, PBA) containing hydrophilic PHEMA moieties (poly(hydroxyethylmethacrylate)). This copolymer tends to self-organize in micelles whose size fits the crystalline structure of PVDF, which is a key parameter for the homogeneous dispersion of the copolymer in the matrix.[25] Direct observation of the hydrophilic layer decorating the very edge of the pores is made possible in transmission electron microscopy by embedding the porous structure in a solid cross linked matrix and selectively staining the hydrophilic additives. This study strongly supports the surface modification approach using segregation effect during the phase inversion process of porous membrane preparation.[26] In a more industrial point of view, it also opens the way to characterize the long-term evolution of fouling resistant porous membranes.

## 2. Experimental Section

### 2.1. Materials and Sample Preparation

**Materials.** The PVDF and the diblock copolymer poly(BA-*co*-HEMA)–*block*–PMMA, referred to as **DB**, 75 wt% PMMA, 20 wt% PBA, 5 wt% HEMA, were kindly provided by ARKEMA. The copolymer was manufactured using ARKEMA internal technology of nitroxide-mediated controlled radical polymerization. The diblock copolymer is synthesized by first preparing the hydrophilic acrylic P(BA-*co*-HEMA) block and then building the second and longer PMMA block. Solvent and residual monomers are then devolatilized. N-methylpyrrolidone (NMP) and polyvinylpyrrolidone (PVP) were purchased from Aldrich and Fluka, respectively.

**Hollow fiber membranes** were manufactured by POLYMEM. Two asymmetric PVDF hollow fiber membranes, containing PVP alone or PVP+**DB**, were fabricated in a dry–wet spinning process. In order to assess the benefit of **DB**, the two membranes were made in similar conditions, only the presence or not of **DB** differed. The two hollow fiber membranes were rinsed in the same conditions, and then were stored in a 50/50 wt% water/glycerol solution.

**Porous planar membranes.** Blend membranes containing PVDF, PVP and/or **DB** copolymer were prepared by casting polymer solutions of 30 wt% solid in NMP after continuous stirring at 80 °C overnight (PVDF/ PVP, 67/33 wt%; PVDF/ **DB**, 50/50 wt%; PVDF/PVP/**DB,** 42/33/25 wt%). The collodions were spread on a glass template using a 5µm-depth casting knife followed by coagulation in water. Then the membranes were washed with water and dried in a vacuum oven at 25 °C overnight.

**Preparation of porous membranes for optical and transmission electron microscopies.** Porous membranes were embedded in Agar resin (low viscosity resin R1078) prepared after the following recipe: LV resin 4.8 g, VH1 hardener 2.6 g, VH2 hardener 2.6 g, accelerator 0.25 mL, then cross linked at 60 °C for 15h.

### 2.2. Characterizations

**Permeability tests.** Pure water permeability was measured at room temperature by plotting water flux for three constant pressures of 0.3, 0.5 and 1 bar following the standard NFX45-101, in manufactured mini-modules comprising 16 hollow fibers of 25 cm which develop an outer surface of 90 $cm^2$. Integrity was checked before and after the permeability measurements.

**Tensile tests.** Strength at break was measured using a tensile strength test device from Mecmesin. A 10-cm fiber sample was pulled between two holders at a speed rate of 350 mm/min. One holder was connected to tensile gauge 0-50 N. Strength at break was measured as the last strength value measured by the gauge before the fiber breaks. The value measured in N was normalized by the fiber section.

**Pressure measurements.** Burst pressure was measured with a bubble point measurement device. One-meter length of hollow fiber was potted at its two ends into two small tubes with an epoxy resin and then pressurized in its lumen with nitrogen at various pressures and increasing steps of 1

bar. Each pressure step was applied during 10 min. Burst pressure was measured as the pressure where a first large breach, with significant $N_2$ bubbles leakage, was observed.

**Attenuated total reflection (ATR)-FTIR measurements.** Spectra were recorded using a Bruker-Tensor 37 FT-IR spectrophotometer equipped with a Gold engate ATR accessory, 4 $cm^{-1}$ resolution.

**Optical microscopy.** Transmitted light bright-field and phase contrast observations were performed using a Leica Leitz DMR microscope. Sections of few micrometers (3 to 10 μm) thickness were cut from the fiber included in resin using a Leica RM 2265 rotary microtome.

**Scanning electron microscopy (SEM).** Fibers were cryo-fractured using liquid nitrogen. Samples were sputter-coated with gold/palladium prior to observation. The morphology of fracture fiber surface was observed using a FEI Magellan 400 microscope operating at 5 or 10 kV. Images of the fiber outer surface were obtained using a Hitachi S4800 instrument operating at 15 kV. The pore size distribution was determined by processing the SEM images obtained with a magnification of x50000 using the ImageJ software.

**Transmission electron microscopy (TEM).** Membrane morphologies were observed using a CEM 902 Zeiss microscope operating under a voltage acceleration of 80 kV. Thin sections (~ 50 nm) were cut at −100 °C using an ultra-cryomicrotome (Leica Ultracut) from membranes embedded in resin, and then stained within $RuO_4$ vapors for 1 min.

**Small Angle X-Ray Scattering (SAXS).** SAXS curves were acquired at the SOLEIL synchrotron facilities, France, using the SWING beam line, wavelength $\lambda$ = 0.83 Å. The sample-CCD camera distance was 4.53 m, the $q$ range 0.03 to 2 $nm^{-1}$.

## 3. Results and discussion

**Porous hollow fibers.** Figure 1 compares various macroscopic characteristics of PVDF hollow fibers containing PVP and **DB**, or only PVP, a classical additive to control the size and homogeneity of the pore formation. PVP also provides some hydrophilicity to the fiber, a property which is lost overtime as the hydrophilic polymer is removed during use and wash processes. Both fibers present similar dimensions and are well concentric. It is remarkable that the macroscopic properties of the fibers are not altered by the presence of the copolymer. Permeability, tensile strength or burst pressure are measured as high in presence of **DB** as with PVP alone. The

amphiphilic copolymer thus may be introduced in the PVDF-PVP hollow fibers with no need for modification of the industrial fabrication process. Subsequently, the new fibers are tested in real conditions of used water filtration. Due to the presence of the copolymer anchoring the hydrophilic block in the matrix, improved properties are expected from the new fibers at the nanoscale.

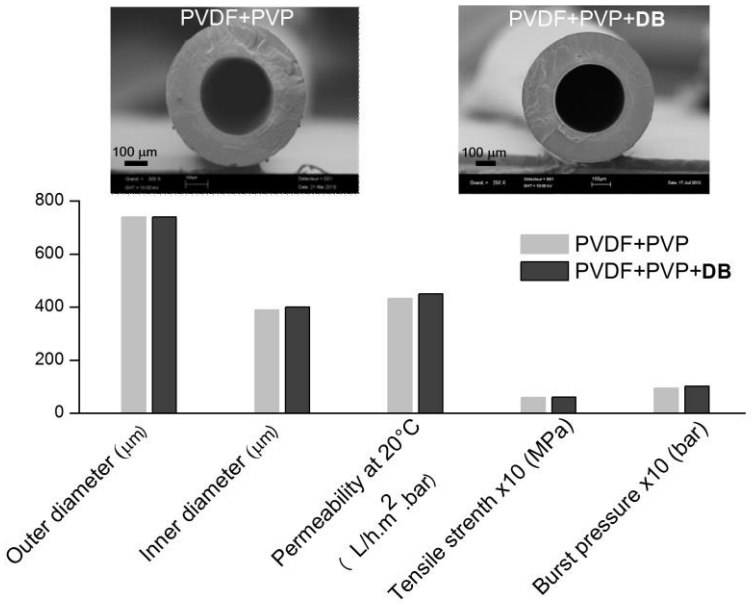


Figure 1. Fiber diameters, pure water permeability, tensile strength at break, and burst pressure when applying pressure in the lumen of PVDF industrial hollow fibers containing PVP or PVP+**DB**.

Figure 2 shows the porous architecture of the hollow fiber membranes as observed by scanning electron microscopy after cryo-fracture. The cross-section of fibers containing either PVP or both additives exhibits a rather homogeneous porous structure with no macro-void formation. The pore size is somewhat larger in the inner side (Figure 2A1, B1) which was expected because the dry-wet spinning parameters were chosen to make denser the outer skin fiber. The pore shape seems to be influenced by the nature of the additives. For membranes containing both additives, pore structure appears mostly as pillars, instead of more regular and planar walls in case of PVP alone (Figure 2A3 and B3).

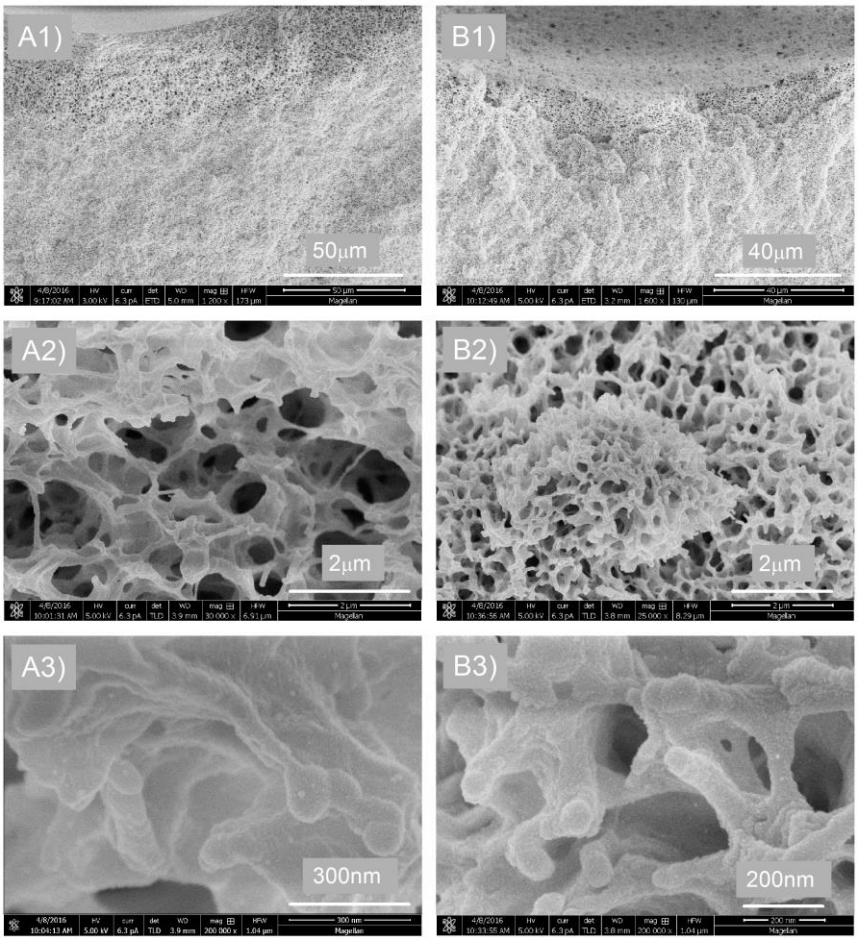


Figure 2. SEM micrographs at three different magnifications of hollow fibers after cryo-fracture containing A) PVDF+PVP; B) PVDF+PVP+**DB**.

SEM observation of the outer fiber surfaces indicates that much smaller pores were obtained using a formulation including both additives (PVP+**DB**) (Figure 3). It was then assumed that the **DB** copolymer induces a drastic change on the phase separation of PVDF. Computerized image analysis was applied for determining the pore diameter distribution (Figure 3C). It can be seen that **DB** acts on two levels: first the decrease of the mean pore size outlined above and second a narrowing of the distribution indicating a marked impact on the interface between the rich and the poor polymer phase.

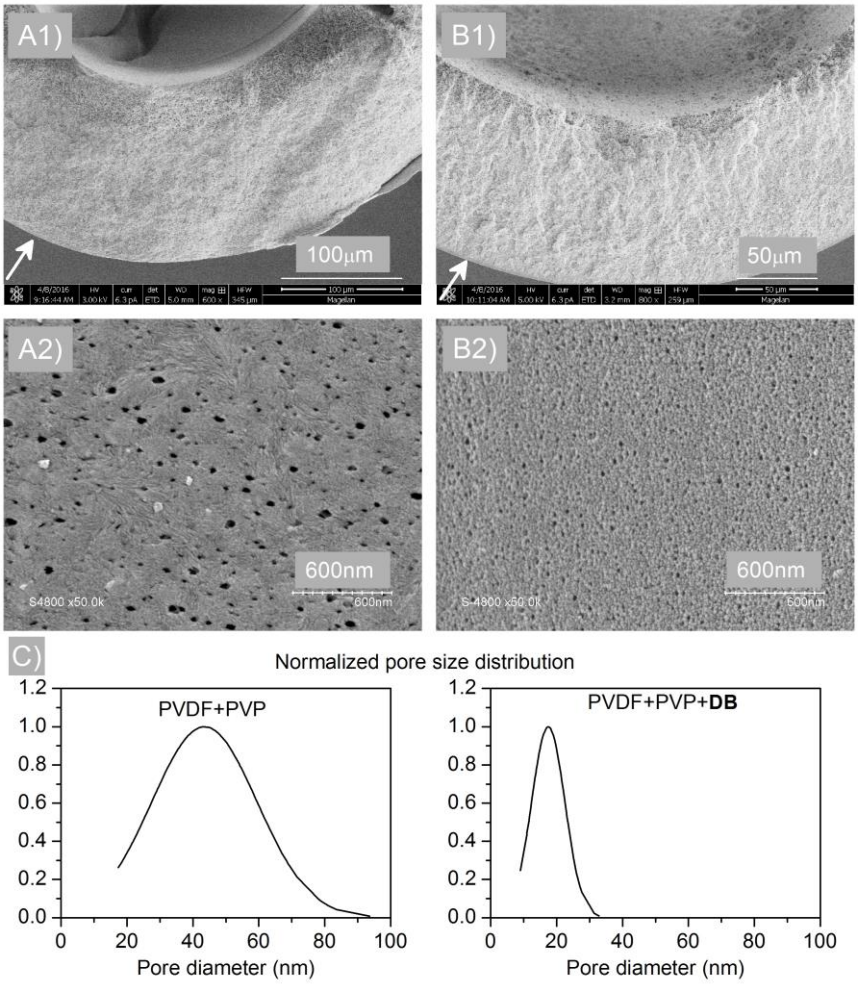


Figure 3. SEM observation of the fibers A) PVDF+PVP, B) PVDF+PVP+**DB**. A1) and B1) after cryo-fracture, showing the inner and outer (pointed out by arrows) surfaces. A2) and B2) visualization of pores on the outer surface. C) Pore diameter distribution determined from SEM observations.

However, SEM does not provide magnification high enough to allow visualization of additives in the fibers. We previously used transmission electron microscopy to observe dense PVDF films containing a copolymer of similar composition.[25] Ultrathin sections were stained with $RuO_4$ vapors, darkening selectively the copolymer. These experiments revealed that in dense films the copolymer preserved its self-organization, while being confined within the lamellar gallery of PVDF, giving rise to a swelling of the crystalline/amorphous lamellar morphology. In the present case of delicate hollow fibers, the preparation of such ultra-thin (50 nm) sections is challenging. Moreover, once the slices prepared, observation of pore contours in TEM is blurred by the presence of the voids skewing the electron contrast.

To overcome these issues, we developed a method to fill in the pores with a solid and transparent material. Inspired by technics used by biologists for observing cellular objects, we embedded the fibers in a thermally cross linkable mixture of resin monomers. Optical micrographs of cross sections of resulting embedded fibers are presented in Figure 4. The overall shape of the fiber is mostly unchanged after embedding, apart from being somewhat flattened (Figure 4A1, B1). The fiber asymmetry appears here more clearly than previously in SEM images (Figure 2). Using the phase contrast mode (Figure 4A2, B2), different zones appear. Between the two bright skins bordering the fiber, three areas may be distinguished: pores in zone 2 appear larger that in zones 1 and 3. The distribution of the three zones is affected by the presence of the additives. In fibers containing both additives, the larger pores are closer to the inner side of the membrane. This may be related to respective interactions of PVP and **DB** with solvent and non-solvent during the inversion phase process of fiber fabrication.

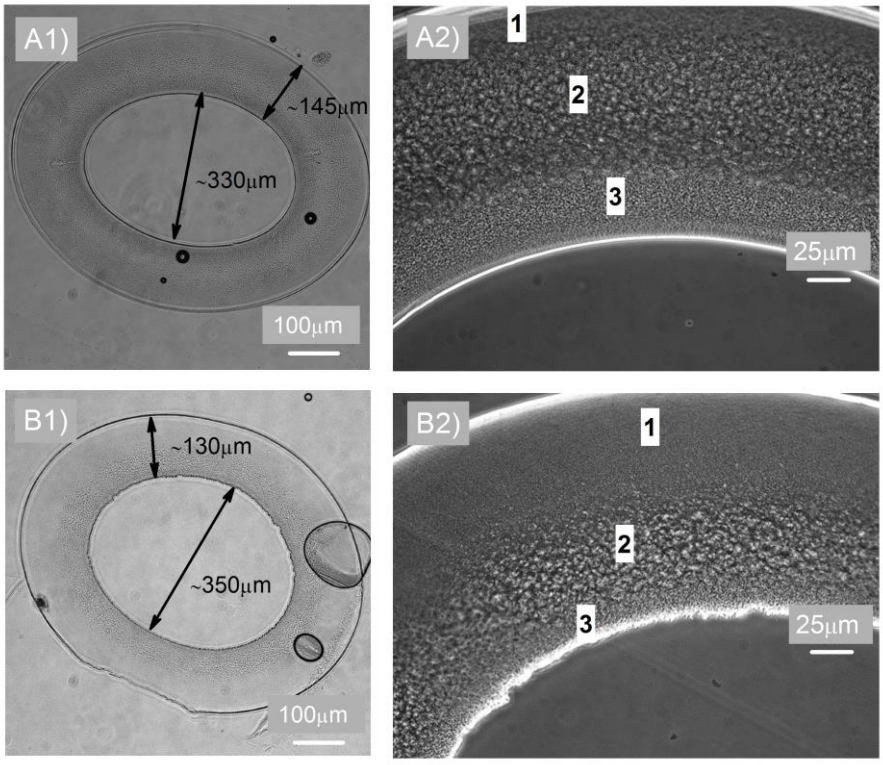


Figure 4. Optical microscopy of hollow fibers embedded in resin containing A) PVDF+PVP; B) PVDF+PVP+**DB.** Left: transmission bright-field images. Right: observation in phase contrast mode.

The resin-reinforced fibers were cut by cryo-ultramicrotomy and the ultra-thin sections stained with $RuO_4$ vapors. Ruthenium tetroxide selectively stains the hydrophilic block, enabling to detect not only the presence of the copolymer but also the possible structuration of the diblock copolymer. **DB** copolymer is composed of two immiscible blocks whose self-structure appears when cast from a NMP solution. As clearly seen in the TEM image of Figure 5, a film of **DB** copolymer exhibits a nano-phase separation between blocks, which will be called micellar structure in the following: stained domains of ~ 6 nm diameter are dispersed in a clearer PMMA matrix. The smaller hydrophilic PBA block containing HEMA moieties, selectively marked by $RuO_4$, assembles in cores appearing darker in the image. The average inter-core distance estimated after the image is ~ 20 nm. In SAXS spectra of copolymer cast films, a unique characteristic distance appears that may be associated to the inter-core distance, as underlined by the scheme of the micelles (Figure 5). This peak measured at $q \sim 0.27$ nm$^{-1}$ corresponds to a 23.5 nm period, supporting the TEM observation.

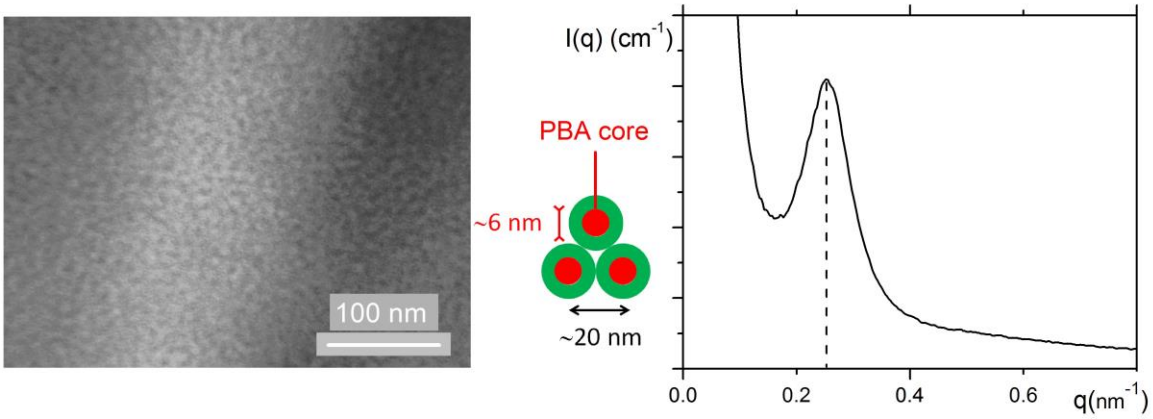


Figure 5. Nanostructure of a **DB** copolymer film cast from NMP. On the TEM image, the hydrophilic blocks assembled in cores appear darker. On the SAXS spectrum, a single signal appearing at 0.27 nm$^{-1}$ corresponds to the average inter-core distance of 23.5 nm.

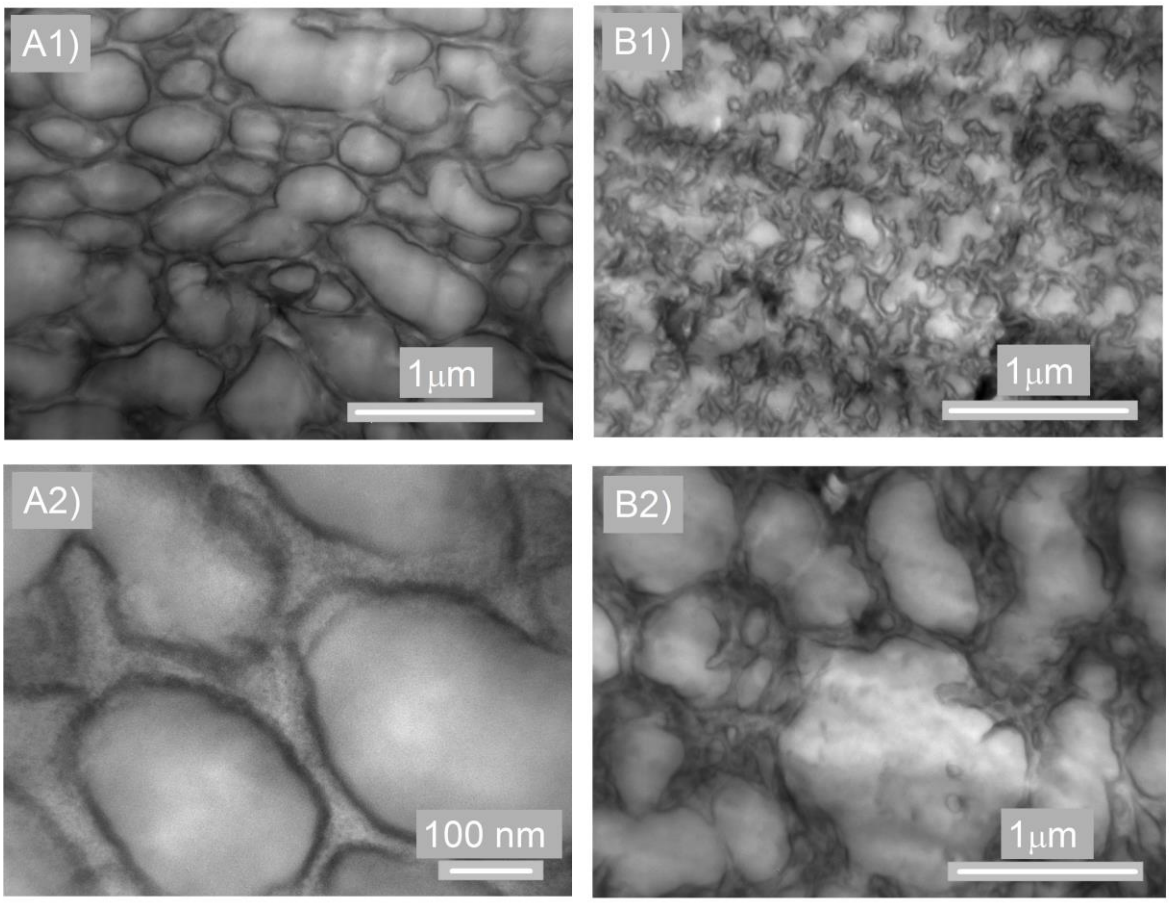


Figure 6. TEM micrographs of hollow fiber embedded in resin. A) PVDF+PVP; B) PVDF+PVP+**DB** at 1, 2: different locations inside the fiber.

According to the above explanation, darker domains in TEM images may be associated to the presence of the copolymer, more precisely to the poly(BA-*co*-HEMA) block. Figure 6 shows the morphology of stained sections of embedded hollow fibers containing only PVP (Figure 6A) or PVP and copolymer (Figure 6B). Clear zones showing almost no contrast correspond to the pores filled by the resin. Darker zones around the pores correspond to the fiber skeleton. Pores of sizes comprised in between 0.1 and 10 μm may be observed all through the fiber thickness, except at the vicinity of the outer surface where sizes are nano-metric. As in the SEM image (Figure 2), the internal structure of the pores appears more tortuous in the case of fibers containing both additives. In the TEM images, the pore contours are clearly underlined by narrow black lines that can be associated to the presence of copolymer. However such black lines surrounding the pores appear as well in the sample containing no copolymer, but only PVP (Figure 6A). This proves that the $RuO_4$ vapors also stain the PVP used in the fiber preparation as a porogen additive. It is

therefore presumable that the black lines in Figure 6B may be associated with both PVP and copolymer. To differentiate both contributions, planar porous membranes were prepared as a model for the internal organization of the hollow fibers.

**Porous planar membranes.** These lab membranes allow for an easier adjustment of the quantity of additives than in case of the hollow fibers industrially prepared. The presence of PVP and/or the copolymer in the membrane after coagulation is attested in infra-red spectra (Figure 7). The appearance of a carbonyl peak around 1665 $cm^{-1}$ in Figure 7B is associated to the amide group of PVP. In planar membranes containing both PVP and **DB**, the peak at 1730 $cm^{-1}$ attributed to the copolymer carbonyl group shows that both amphiphilic additives are integrated in the membrane after coagulation (Figure 7D).

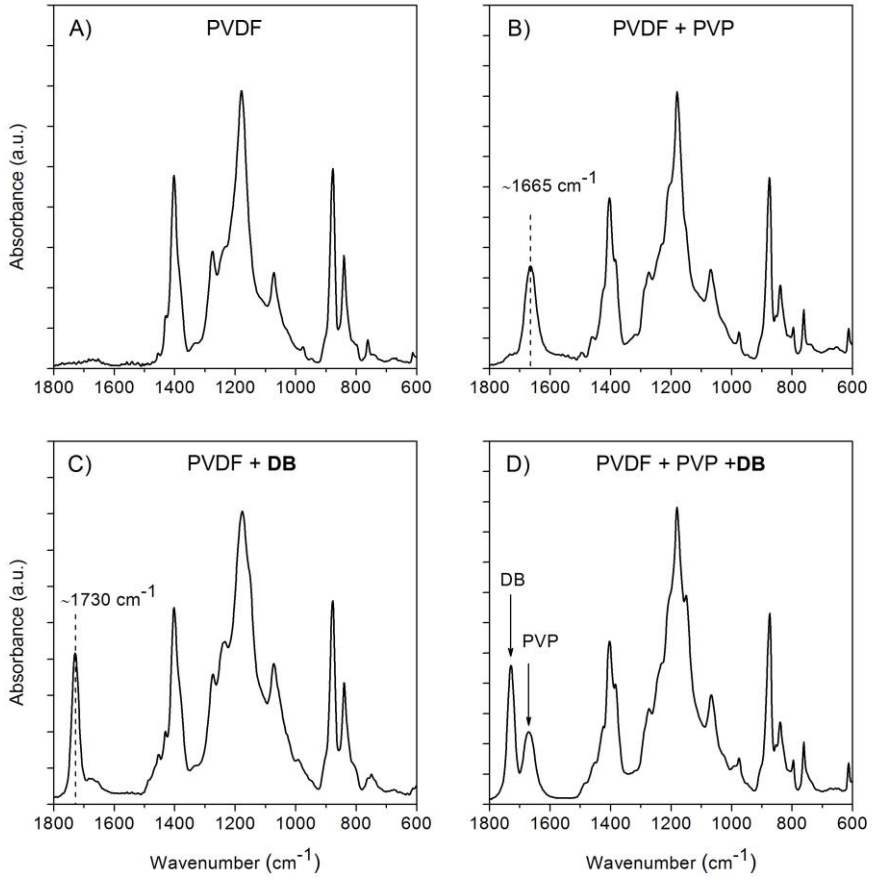


Figure 7. ATR-IR spectra of porous planar membranes. A) PVDF; B) PVDF+PVP; C) PVDF+**DB**; D) PVDF+PVP+**DB**.

Figure 8 shows TEM images of ultrathin sections of planar porous membranes after staining with $RuO_4$. In Figure 8A is presented a view of a **DB** containing membrane which has not been embedded in resin. Dark lines surrounding the pores might be associated to the presence of the copolymer at their surface. However, the strong contrast brought by the voids affects the readability of the image. As for fibers, the planar porous membranes were embedded in resin for a better observation. Figure 8B shows the image of a PVDF membrane containing PVP. Pores full of resin appear as clear areas surrounded by a black line that is attributed to stained PVP. Planar PVDF membranes fabricated without PVP display a less controlled but still porous structure (Figure 8C). The poor contrast of this image could not be improved, neither by TEM settings nor image adjustments. The $RuO_4$ is not expected to stain specifically the PVDF. The homopolymer nevertheless appears darker than the resin, owing to the presence of heavy fluorine atoms that may interact with electron beam more than components of the organic resin. Still, despite the low contrast, there is no doubt that the clear zones corresponding to the pores are not surrounded by black lines. The surface dark lines when observed could therefore be attributed to the presence of the additives. Figure 8D shows the morphology of a porous PVDF membrane containing **DB**, prepared without PVP. Contours of the pores are decorated with dark lines, which here are associated with the presence of the sole copolymer, preferentially located on the pore surface after the inversion phase process. This surface enrichment process however does not prevent the copolymer to be present in bulk, as supported by the contrast observed in the PVDF matrix, highly enhanced as compared to Figure 8C. In Figure 8D the semi-crystalline structure of PVDF clearly shows up. Because the copolymer incorporates the amorphous domains in the lamellar gallery of the semi-crystalline homopolymer, the result is a better contrast in the crystalline zones of the images, as already observed in dense films.[25]

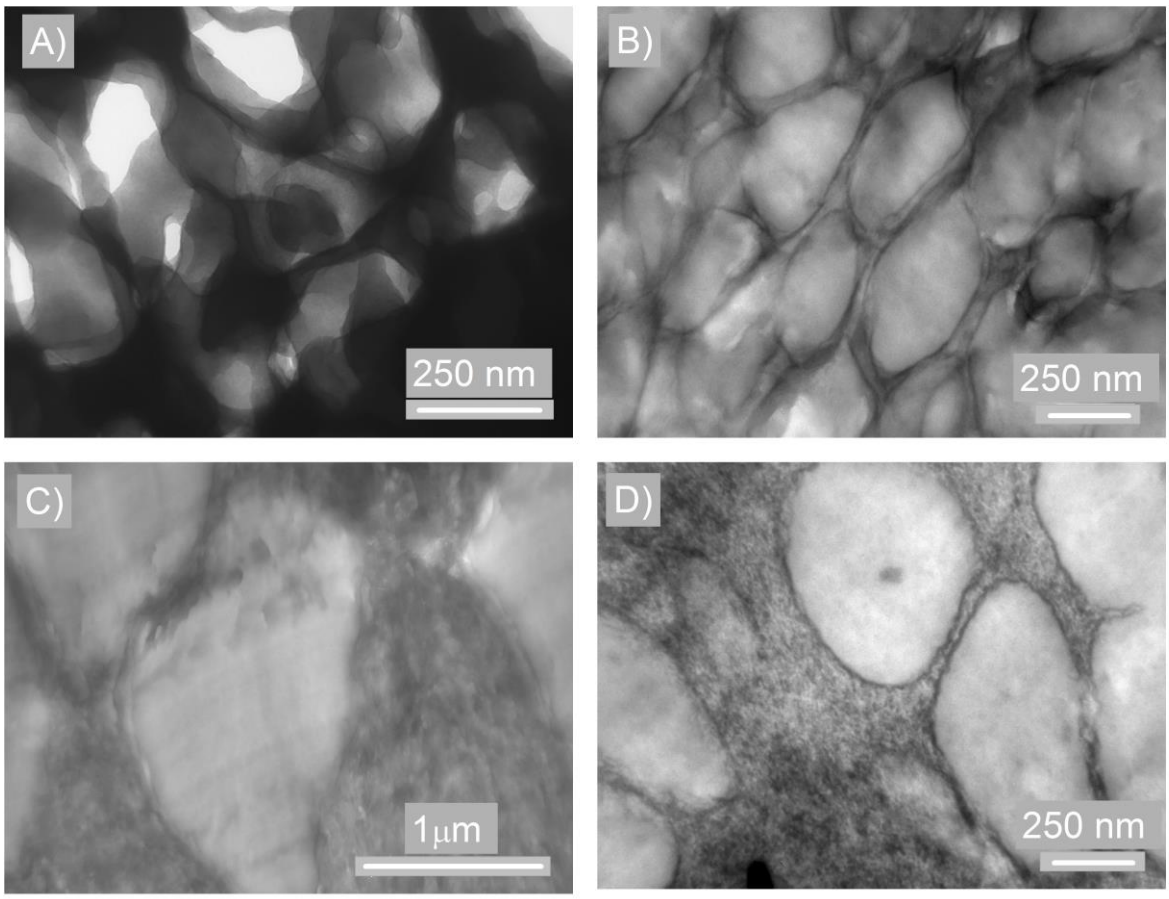


Figure 8. TEM images of porous planar membranes, A) PVDF+**DB**, no resin; B-D) embedded in resin: B) PVDF+PVP; C) PVDF only; D) PVDF**+DB**.

The planar porous membranes model thus brings the first evidence of the localization of a hydrophilic additive on the pore surface of a hollow fiber membrane. Transmission electron microscopy of samples embedded in resin and stained with ruthenium tetroxide appears as a valuable methodology to characterize the efficiency of surface enrichment by hydrophilic additives.

Moreover, with our system, as the diblock copolymer is well entrapped in the lamellar gallery of the semi-crystalline polymer, a good anchoring of the fouling resistant agent in the PVDF matrix is expected. This guest-host cooperative interaction results from the molecular size of the self-organizing copolymer. As said previously, micelles of the amphiphilic **DB** copolymer are trapped in the amorphous lamellae of PVDF in dense films.[25] As schematized in Figure 9A, the interlamellar long distance $L_p$ of the semi-crystalline polymer increases from 120 Å up to more

than 200 Å, according to the content of added copolymer. A TEM image of such intimate mixing of PVDF and nanostructured **DB** copolymer is provided in Figure 9B. The semi-crystalline lamellar structure of PVDF is preserved but swelled by the **DB** micelles whose size fits the PVDF long period. This $L_p$ increase was already observed in presence of a hydrophilic immiscible polymer when mixed with a counter-ion acting as miscibility agent with the PVDF matrix.[27] In the present study, the PMMA block miscible with PVDF plays the role of intercessor to integrate the immiscible hydrophilic block in the bulk matrix. Miscibility of PMMA and PVDF should in addition favor stabilization of the amphiphilic additive at the surface of the pores (Figure 9C).

The PVP is not drawn in Figure 9C. As ternary blends of PVDF/PVP/PMMA were reported to be miscible,[28] the question arises as to whether the presence of the copolymer could have a positive effect on the stabilization of hydrophilic PVP itself in membranes containing both additives. Not only the PVP could incorporate the lamellar gallery of the PVDF at the inversion phase step, but also its leaching under repetitive cleaning procedures could be minimized. Further studies to differentiate PVP and the copolymer at the microscopic scale are in progress. Fate of these hydrophilic additives in hollow fiber membranes in use for water filtration is currently under investigation.

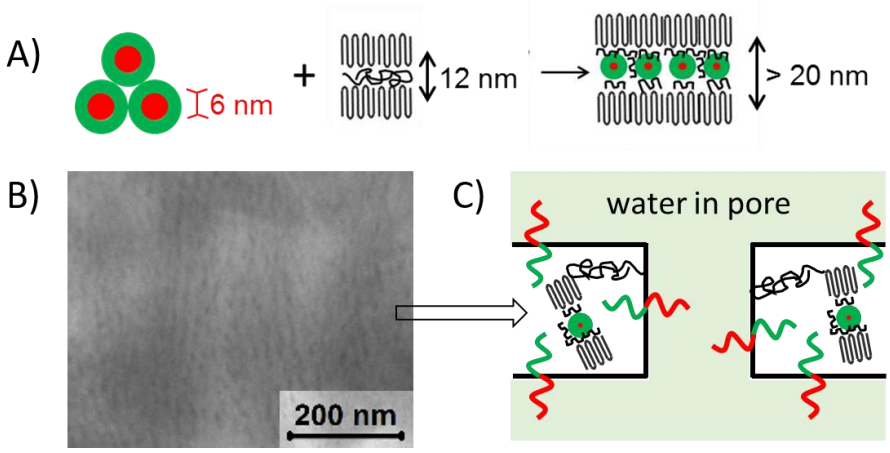


Figure 9. Compatibility of PVDF and **DB** copolymer. Black: PVDF; Green: PMMA; Red: Hydrophilic block. A) In bulk membranes, the self-organizing copolymer integrates the amorphous layers of PVDF; B) TEM image of dense PVDF film containing **DB** (after [25]); C) Scheme of pore surface. PMMA miscible with PVDF may help to anchor the hydrophilic block at the pore surface.

## 4. Conclusion

Industrial hollow fibers aimed at the purification of wastewater were fabricated by adding to a standard PVDF/PVP formulation an amphiphilic diblock copolymer. The initial macroscopic properties of the hollow fibers were not altered by the presence of the copolymer. Observation of the fiber pore structure by transmission electron microscopy was made possible by embedding the fibers into a resin that filled in the voids. It was shown that both hydrophilic additives were located all around the pores, where however they could not be differentiated. It is the first direct proof at the microscopic scale of pore surface enrichment by antifouling agents. Model porous planar membranes containing only the copolymer demonstrated that the amphiphilic additive located specifically around the pores. As the copolymer contains a PMMA block miscible with PVDF that may act as anchor in the fiber matrix, it is expected that the amphiphilic additive resist longer than PVP to multiple washing procedures. To investigate this beneficial effect in hollow fibers, accelerated chemical ageing as well as studies to differentiate PVP and the copolymer by specific staining are currently in progress.

**Acknowledgements.** This work was supported by the Fond Unique Interministériel (FUI) funded by BPI France, through the NEOPHIL project. Authors acknowledge SOLEIL, France, for providing synchrotron radiation facilities, Dr Michel Glotin and Dr Pierre Gérard (Arkema) for their contribution at the early stages of this work.

## References

[1] F. Liu, N. Awanis Hashim, Y. Liu, M.R. Moghareh Abed, K. Li, Progress in the production and modification of PVDF membranes, J. Membr. Sci. 375 (2011) 1–27.

[2] G.-D. Kang, Y.-M. Cao, Application and modification of poly(vinylidene fluoride) (PVDF) membranes – A review, J. Membr. Sci. 463 (2014)145–165.

[3] S. Nishigochi, T. Ishigami, T. Maruyama, Y. Hao, Y. Ohmukai, Y. Iwasaki, H. Matsuyama, Improvement of antifouling properties of polyvinylidene fluoride hollow fiber membranes by

simple dip coating of phosphorylcholine copolymer via hydrophobic interactions, Ind. Eng. Chem. Res. 53 (2014) 2491–2497.

[4] A. Venault, Y. Chang, H.S. Yang, P.Y. Lin, Y.J. Shih, A. Higuchi, Surface self-assembled zwitterionization of poly(vinylidene fluoride) microfiltration membrane via hydrophobic-driven coating for improved blood compatibility, J. Membr. Sci. 454 (2014) 253–263.

[5] J.R. Du, S. Peldszus, P.M. Huck, X. Feng, Modification of poly(vinylidene fluoride) ultrafiltration membranes with poly(vinylalcohol) for fouling control in drinking water treatment, Water Res. 43 (2009) 4559–4568.

[6] Y.-C. Chiang, Y. Chang, A. Higuchi, W.-Y. Chen, R.-C. Ruaan, Sulfobetaine-grafted poly(vinylidene fluoride) ultrafiltration membranes exhibit excellent antifouling property, J. Membr. Sci. 339 (2009) 151–159.

[7] Y. Sui, X. Gao, Z. Wang, C. Gao, Antifouling and antibacterial improvement of surface-functionalized poly(vinylidene fluoride) membrane prepared via dihydroxyphenylalanine-initiated atom transfer radical graft polymerizations. J. Membr. Sci. 394–395 (2012) 107–119.

[8] M.G. Zhang, Q.T. Nguyen, Z.H. Ping, Hydrophilic modification of poly(vinylidenefluoride) microporous membrane, J. Membr. Sci. 327 (2009) 78–86.

[9] Y. Chang, C.-Y. Ko, Y.-J. Shih, D. Quémener, A. Deratani, T.-C. Wei, D.-M. Wang, J.-Y. Lai Surface grafting control of PEGylated poly(vinylidene fluoride) anti-fouling membrane via surface-initiated radical graft copolymerization, J. Membr. Sci. 345 (2009) 160–169.

[10] T. Cai, K.G. Neoh, E.T. Kang, Poly(vinylidene fluoride) graft copolymer membranes with "clickable" surfaces and their functionalization, Macromolecules 44 (2011) 4258–4268.

[11] W.Z. Lang, Z.L. Xu, H. Yang, W. Tong, Preparation and characterization of PVDF–PFSA blend hollow fiber UF membrane, J. Membr. Sci. 288 (2007)123–131.

[12] S.-H. Zhi, J. Xu, R. Deng, L.-S. Wan, Z.-K. Xu, Poly(vinylidene fluoride) ultrafiltration membranes containing hybrid silica nanoparticles: Preparation, characterization and performance, Polymer 55 (2014) 1333–1340.

[13] X. Zhao, H. Xuan, Y. Chen, C. He, Preparation and characterization of superior antifouling PVDF membrane with extremely ordered and hydrophilic surface layer, J. Membr. Sci. 494 (2015) 48–56.

[14] N. Singh, S.M. Husson, B. Zdyrko, I. Luzinov, Surface modification of microporous PVDF membranes by ATRP, J. Membr. Sci. 262 (2005) 81–90.

[15] Y. Chen, Q. Deng, J. Xiao, H. Nie, L. Wu, W. Zhou, B. Huang, Controlled grafting from poly(vinylidene fluoride) microfiltration membranes via reverse atom transfer radical polymerization and antifouling properties, Polymer 48 (2007) 7604–7613.

[16] J.F. Hester, P. Banerjee, Y.-Y. Won, A. Akthakul, M.H. Acar, A.M. Mayes, ATRP of amphiphilic graft copolymers based on PVDF and their use as membrane additives, Macromolecules 35(2002) 7652–7661.

[17] F. Liu, Y.-Y. Xu, B.-K. Zhu, F. Zhang, L.-P. Zhu, Preparation of hydrophilic and fouling resistant poly(vinylidene fluoride) hollow fiber membranes, J. Membr. Sci. 345 (2009) 331–339.

[18] J.F. Hester, A.M. Mayes, Design and performance of foul-resistant poly(vinylidene fluoride) membranes prepared in a single-step by surface segregation, J. Membr. Sci. 202 (2002) 119–135.

[19] D. Liu, D. Li, D. Du, X. Zhao, A. Qin, X. Li, C. He, Antifouling PVDF membrane with hydrophilic surface of terrypile-like structure, J. Membr. Sci. 493 (2015) 243–251.

[20] Y. Liu, Y. Su, Y. Li, X. Zhao, Z. Jiang, Improved antifouling property of PVDF membranes by incorporating an amphiphilic block-like copolymer for oil/water emulsion separation, RSC Adv. 5 (2015) 21349–21359.

[21] Y.-H. Zhao, B.-K. Zhu, L. Kong, Y.-Y. Xu, Improving hydrophilicity and protein resistance of poly(vinylidene fluoride) membranes by blending with amphiphilic hyperbranched-star polymer, Langmuir 23 (2007) 5779–5786.

[22] A. Venault, Y.-H. Liu, J.-R. Wu, H.-S. Yang, Y. Chang, J.-Y. Lai, P. Aimar, Low-biofouling membranes prepared by liquid-induced phase separation of the PVDF/polystyrene-b-poly(ethyleneglycol) methacrylate blend, J. Membr. Sci. 450 (2014) 340–350.

[23] Z. Yao, Y. Cui, K. Zheng, B. Zhu, L. Zhu, Composition and properties of porous blend membranes containing tertiary amine based amphiphilic copolymers with different sequence structures, J. Coll. Int. Sci. 437 (2015) 124–131.

[24] E. Dufour, S. Gassara, E. Petit, C. Pochat-Bohatier, A. Deratani, Quantitative PVP mapping in PVDF hollow fiber membranes by using Raman spectroscopy coupled with spectral chemiometrics analysis, Eur. Phys. J. Special Topics 224 (2015) 1911–1919.

[25] E.K. Oikonomou, S. Tencé-Girault, P. Gérard, S. Norvez, Swelling of semi-crystalline PVDF by a PMMA-based nanostructured diblock copolymer: Morphology and mechanical properties, Polymer 76 (2015) 89–97.

[26] J.F. Hester, P. Banerjee, A.M. Mayes, Preparation of protein-resistant surfaces on poly(vinylidene fluoride) membranes via surface segregation, Macromolecules 32 (1999) 1643–1650.

[27] C.M. Gibon, S. Norvez, S. Tencé-Girault, J.T. Goldbach, Control of morphology and crystallization in polyelectrolyte/polymer blends, Macromolecules 41 (2008) 5744–5752.

[28] J. Cheng, S. Wang, S. Chen, J. Zhang, X. Wang, Crystallization behavior and hydrophilicity of poly(vinylidene fluoride)/poly(methylmethacrylate)/poly(vinyl pyrrolidone) ternary blends, Polym. Int. 61 (2012) 477–484.